



A robust approximation method for nonlinear cases of structural reliability analysis



Mohammad Amin Roudak^{a,*}, Mohsen Ali Shayanfar^b, Mohammad Ali Barkhordari^a, Mohammad Karamloo^c

^a School of Civil Engineering, Iran University of Science and Technology, Narmak, Tehran 16846, Iran

^b The Centre of Excellence for Fundamental Studies in Structural Engineering, Iran University of Science and Technology, Narmak, Tehran 16846, Iran

^c Department of Civil Engineering, Shahid Rajae Teacher Training University, Lavizan, Tehran, Iran

ARTICLE INFO

Keywords:

Reliability index
Generalization of HL-RF
Adjusting parameters
Nonlinear limit state function

ABSTRACT

The Hasofer–Lind and Rackwitz–Fiessler (HL-RF) method is a popular iterative approximation method in structural reliability analysis. However, it may pose numerical instability and result in divergence in the face of high nonlinearity. In the present paper, two adjusting parameters are included in this method and a generalization of HL-RF is proposed. The represented parameters are to control the convergence of the sequence especially when nonlinearity increases. The proposed algorithm actually improves the performance of HL-RF in convergence, while it remains as simple as HL-RF to implement without any need to merit functions or line search processes, needed in many approximation methods. Through various numerical examples, the robustness and efficiency of the proposed algorithm in highly nonlinear cases have been shown.

© 2017 Elsevier Ltd. All rights reserved.

1. Introduction

In structural analysis, examples of uncertainty can be observed in material, load and geometric properties. Thus, uncertainty is of great importance for a realistic analysis [1–3]. Structural reliability theory provides a tool to bring the effects of uncertainty in structural analysis [4–6]. In reliability analysis, evaluation of probability of failure P_f is the main purpose. P_f is mathematically expressed by the following multi-dimensional integral

$$P_f = \int_{g(X) < 0} f_X(X) dX \quad (1)$$

where the vector $X = [X_1, X_2, \dots, X_n]^T$ represents random variables and $f_X(X)$ is the joint probability density function (JPDF) associated with this vector. $g(X)$ is the limit state function (LSF) and is defined such that $g(X) > 0$ and $g(X) < 0$ represent safety and failure domain, respectively. In practice, evaluating the integral of Eq. (1) is a numerical challenge, especially for complex structures or in the cases with low probability of failure and implicit LSFs. The reason of this difficulty is obviously involving multiple integral and JPDF of variables. That is why attentions have been directed to other alternatives such as simulation methods [7–10] and approximation methods [11–14].

Simulation methods, one of which is Monte Carlo simulation (MCS), are based on generating random samples by a sampling density function (SDF). LSF is evaluated for all generated samples. Probability of failure is computed as the ratio of the number of samples regarding failure (negative value of LSF), to total sampling number. Importance sampling (IS) is a useful technique that recognizes more important regions of generating samples [15–17]. Simulation methods are capable of expressing accurate solutions. However, they are dependent on the generation of large number of samples and therefore may not be suitable for practical cases [18–20].

Among approximate methods, first-order reliability method (FORM) has attracted much attention and is widely used in the reliability problems. The main basic method in this class was proposed by Hasofer and Lind [21]. Based on their method, random variables are transformed from the original space (X -space) to the so-called standard normal coordinate system (U -space) by the following transformation

$$u_i = \frac{x_i - \mu_{X_i}}{\sigma_{X_i}} \quad (2)$$

where μ_{X_i} and σ_{X_i} are mean and standard deviation of i th random variable, respectively. Besides, they proposed to approximate the LSF (denoted by G in U -space) using Taylor expansion at design point or most probable point (MPP). This point, according to the definition of Hasofer and Lind, is a point on limit state surface with the minimum distance

* Corresponding author.

E-mail addresses: amin_roudak@civileng.iust.ac.ir, aminroudak@yahoo.com (M.A. Roudak), shayanfar@iust.ac.ir (M.A. Shayanfar), barkhordar@iust.ac.ir (M.A. Barkhordari), m.karamloo@srttu.edu, karamloo@yahoo.com (M. Karamloo).

from the origin of U -space. This minimum distance is reliability index, denoted by β . The aforementioned Taylor expansion results in an iterative relation for the new design point as

$$U_{k+1} = \frac{\nabla^T G(U_k) U_k - G(U_k)}{\nabla^T G(U_k) \nabla G(U_k)} \nabla G(U_k) \quad (3)$$

where U_{k+1} is the design point of HL-RF at iteration $k+1$, defined in terms of the current design point U_k .

Rackwitz and Fiessler [22] extended the Hasofer–Lind method to take the distribution of random variables into account. For non-normal variables, they proposed to replace the transformation of Eq. (2) with the following transformation

$$u_i = \frac{x_i - \mu'_{X_i}}{\sigma'_{X_i}} \quad (4)$$

in which μ'_{X_i} and σ'_{X_i} are called mean and standard deviation of i th equivalent normal variable, respectively, and are computed by

$$\sigma'_{X_i} = \frac{\varphi\left\{\Phi^{-1}\left[F_{X_i}(x_i^*)\right]\right\}}{f_{X_i}(x_i^*)} \quad (5)$$

$$\mu'_{X_i} = -\sigma'_{X_i} \Phi^{-1}\left[F_{X_i}(x_i^*)\right] + x_i^* \quad (6)$$

where φ and Φ denote probability density function (PDF) and cumulative distribution function (CDF) of standard normal distribution, respectively. $f_{X_i}(x_i^*)$ and $F_{X_i}(x_i^*)$ are the PDF and CDF of the original variable X_i , respectively, at the i th component of design point (i.e. at x_i^*). This method, denoted as HL-RF (Hasofer, Lind–Rackwitz, Fiessler), is widely used in structural reliability problems. However, in nonlinear cases the method could exhibit unstable solutions (by periodic or chaotic behaviors) or it might converge very slowly. Thus, several studies have been carried out to remove these deficiencies. On this way, Liu and Kiureghian [23] proposed a merit function to monitor the convergence trends of the problems. Wang and Grandhi [24] applied intervening variables to improve the performance of HL-RF. This was done by the introduction of a nonlinearity index, which is itself computed through a sub-iterative process at each iteration. Elegbede [25] applied particle swarm optimization for computation of reliability index in the cases of normally distributed variables. Santosh et al. [26] used sub-iterations of Armijo rule at each iteration to select a suitable step size. Yang [27] applied chaos control in his stability transformation method. His algorithm converges very slowly in complicated problems with high nonlinearity. Gong and Yi [28] proposed a method by introducing a search direction and a step length. Gong et al. [29] proposed a non-gradient-based algorithm to locate design point by producing n series of sequence points iteratively in the n -dimensional standard normal coordinate system. There are also other alternatives to be used in the field of reliability analysis. Perturbation technique, for instance, provides a tool which can be used as an alternative [30]. Taylor expansion of LSF, of the general order, using perturbation technique to deal with reliability problems can be found in [31].

In this paper, a reliability algorithm is proposed by providing a new general overview of the approximation methods. This algorithm, which is a generalization of HL-RF, applies two parameters. The introduction of these parameters provides a suitable seedbed for controlling the convergence of the sequences, especially in highly nonlinear cases where HL-RF may have difficulty in convergence. In fact in a specific problem, HL-RF either converges or results in divergence. If HL-RF diverges in a problem there is no adjusting parameter to change and reach convergence, while, the parameters of the proposed algorithm can be adjusted to deal with highly nonlinear problems. For specific values of the applied parameters the proposed method reduces to HL-RF method. Although in some problems these values (corresponding to HL-RF) can work, they must change in many other cases with large nonlinearity degrees. It should be noted that the proposed algorithm, due to its new idea, can work properly only with first-order terms of Taylor expansion and without need to higher

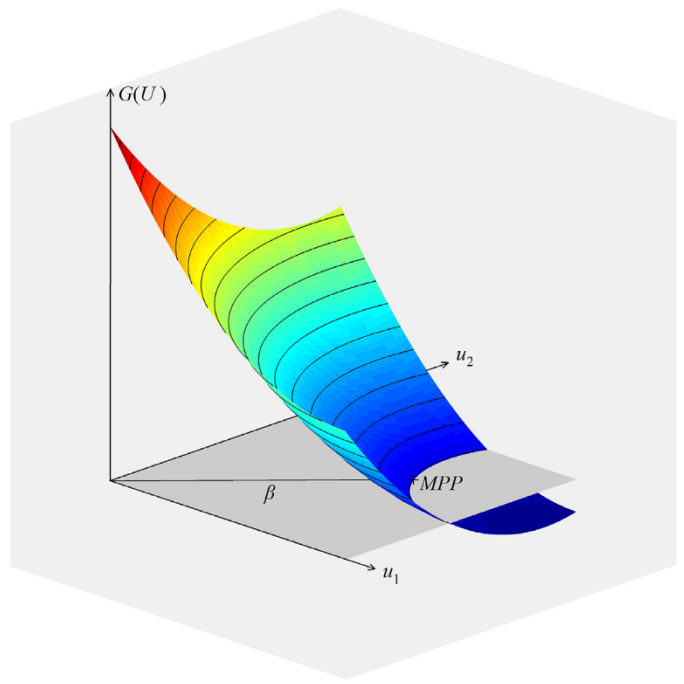


Fig. 1. Schematic description of design point and reliability index for two random variables.

order terms, and therefore the proposed algorithm is as simple as HL-RF while its effectiveness has been improved.

2. Proposed algorithm

As mentioned before, HL-RF does not have any adjusting parameter and therefore in some nonlinear problems this can result in periodic or chaotic behaviors. In this paper two parameters, by which such unstable behaviors can be avoided, are included in HL-RF method and a generalization of HL-RF is obtained. Details and formulation of the proposed algorithm is explained in Section 2.1. The summary of the proposed algorithm is also presented in Section 2.2.

2.1. Details and formulation

As previously mentioned the reliability index β is obtained by minimizing the distance function in n -dimensional space under the constraint $G(U)=0$, i.e. β is the minimum distance of the limit state surface $G(U)=0$ in n -dimensional space from the origin (n corresponds to the domain of n random variables). Suppose, instead of drawing limit state surface $G(U)=0$ in n -dimensional space, the limit state function $G(U)$ is drawn in $(n+1)$ -dimensional space (1 added dimension corresponds to the axis of function G). Thus, β in this $(n+1)$ -dimensional space is obviously the minimum distance of the origin from $G(U)$ at the intersection with plane $G(U)=0$ as the constraint (see schematic illustration of Fig. 1 for $n=2$). It should be noted that the added dimension is just to create the possibility of introducing the first adjusting parameter of the proposed algorithm. Therefore, as it will be explained later, it does not increase the computation dimensions and all formulations will be given in n -dimensional space (like HL-RF).

As it is known, in HL-RF method G is replaced with the tangential plane of G at U_k (this plane is denoted by \bar{G}) using the following linear terms of Taylor expansion

$$G(U_{k+1}) \approx \bar{G}(U_{k+1}) = G(U_k) + \nabla^T G(U_k)(U_{k+1} - U_k) \quad (7)$$

Then the above equation of tangential plane is set to zero, i.e. the intersection of \bar{G} with the plane $G(U)=0$ is considered. The schematic interpretation of these explanations in the $(n+1)$ -dimensional space is

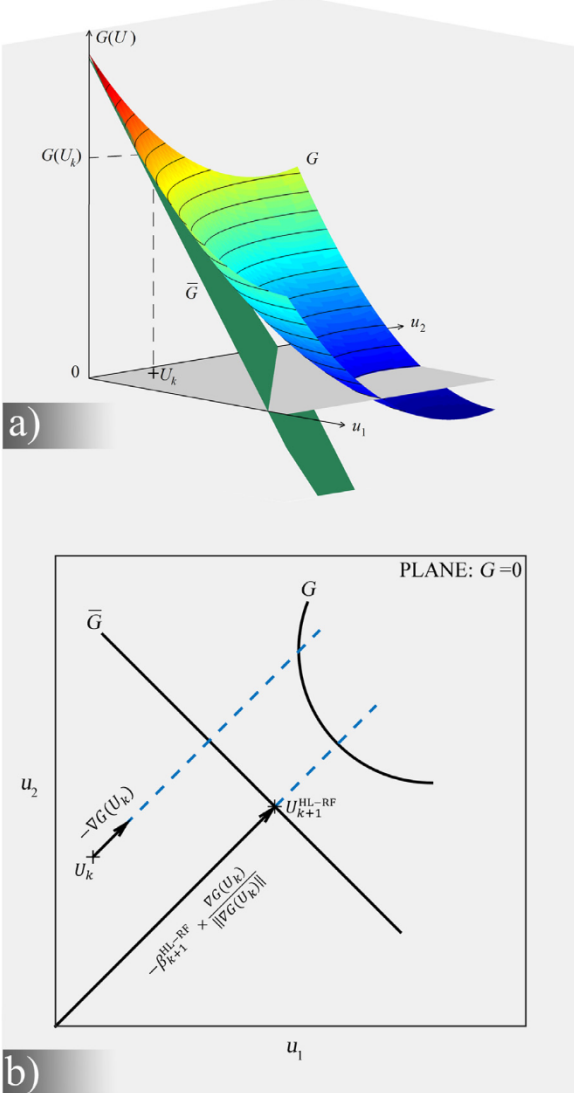


Fig. 2. HL-RF method for two random variables (a) intersection plane $G=0$ (b) determination of the next MPP in the intersection plane.

represented in Fig. 2(a), for $n=2$. Finally, U_{k+1} of HL-RF is obtained as a point on the aforementioned intersection and in the direction of $-\nabla G(U_k)$, as shown in Fig. 2(b).

To explain the first adjusting parameter of the proposed algorithm the following issue should be noticed. Setting the equation of tangential plane equal to zero, in the cases $G(U_k)$ is a lot bigger or smaller than zero, can be potentially a risk for convergence because this causes a sudden and abrupt movement from the plane $G=G(U_k)$ to the plane $G=0$ (see Fig. 2(a)). This can disturb the iterative process especially when the limit state function $G(U)$ is highly nonlinear between these two planes.

To circumvent the possible problem an adjusting parameter γ , by which the aforementioned abrupt movement can be replaced with a gradual movement, is introduced. Hence, to find U_{k+1} , Eq. (8) is proposed as

$$\bar{G}(U_{k+1}) = G(U_k) + \nabla^T G(U_k)(U_{k+1} - U_k) = \gamma G(U_k) \quad (8)$$

in which γ is a constant in the range $[0,1]$. Fig. 3(a) illustrates the effect of γ . In fact in the proposed algorithm the tangential plane \bar{G} will be intersected by the plane $G=\gamma G(U_k)$ instead of $G=0$ (which is used in HL-RF). If γ is selected in the aforementioned range, the tangential plane \bar{G} is intersected by a plane between the plane $G=0$ and the previous

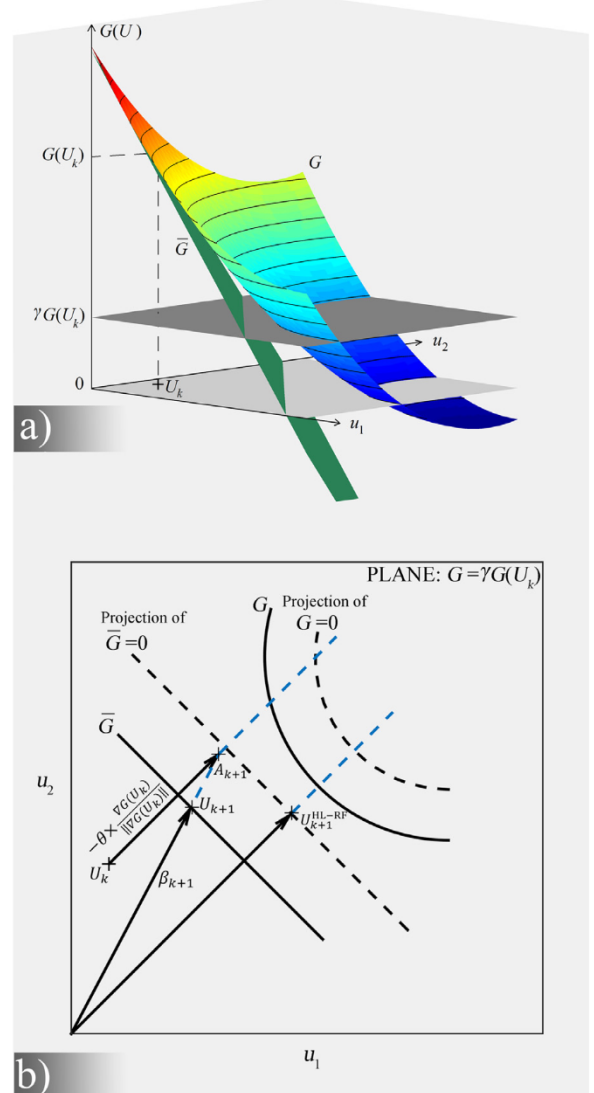


Fig. 3. Proposed algorithm for two random variables (a) determination of the intersection plane using γ , (b) determination of the next MPP in the intersection plane using θ .

plane $G=G(U_k)$, as shown in Fig. 3(a). It should be noted that in the special case of $\gamma=0$ the relation of Eq. (8) reduces to what is used in HL-RF. In this special case, as it can be seen in Fig. 3(a), our introduced intersection plane $G=\gamma G(U_k)$ falls exactly on the intersection plane of HL-RF method $G=0$. The parameter γ , which allows gradual movements towards $G=0$, is one of the adjusting parameters added to HL-RF to improve the performance in highly nonlinear cases.

In contrast to the first adjusting parameter, which considers a step length in the direction of axis G , the second parameter should be explained inside the plane of n random variables. To do so, consider Fig. 3(b) corresponding to the intersection plane $G=\gamma G(U_k)$. According to this figure the tangential plane of Fig. 3(a), i.e. \bar{G} , is a linear function in the aforementioned intersection plane, i.e. in $G=\gamma G(U_k)$. To determine a point on this linear function as U_{k+1} , the direction of U_{k+1} in this intersection plane should be specified. In HL-RF a line is drawn from the origin of the plane and parallel to $-\nabla G(U_k)$, to intersect the linear function (as seen in Fig. 2(b)). This implies that from U_k , a step with infinite length along $-\nabla G(U_k)$ is taken. Then, from the resulted infinitely far point, a line is drawn to pass through the origin of the plane (this line is clearly parallel to $-\nabla G(U_k)$). Where this line intersects the linear function, is U_{k+1} of HL-RF shown in Fig. 2(b).

Suppose, as proposed by Gong and Yi [28], the step length from U_k and in the direction of negative gradient has a finite value instead of infinity. Accordingly, in the proposed intersection plane $G = \gamma G(U_k)$, the so-called auxiliary point A_{k+1} which has been shown in Fig. 3(b) is obtained from U_k as

$$A_{k+1} = U_k - \theta \frac{\nabla G(U_k)}{\|\nabla G(U_k)\|} \quad (9)$$

where the constant θ denotes the step length along $-\nabla G(U_k)$ from U_k . Referring to Fig. 3(b), one can observe that the line connecting the origin of the intersection plane to A_{k+1} is selected as the direction of U_{k+1} . Therefore, the vector of direction cosines of U_{k+1} is

$$V_{k+1} = \frac{A_{k+1}}{\|A_{k+1}\|} \quad (10)$$

It has been shown in Fig. 3(b) that U_{k+1} is a point on this vector and at the intersection with the tangential plane \bar{G} . To reach the point U_{k+1} of Fig. 3(b) we write

$$U_{k+1} = \beta_{k+1} V_{k+1} \quad (11)$$

where β_{k+1} is reliability index at iteration $k+1$. By selecting a value for θ , A_{k+1} of Eq. (9) and V_{k+1} of Eq. (10) can be determined. To compute β_{k+1} and consequently U_{k+1} at the intersection with \bar{G} , Eq. (11) is placed in Eq. (8). In other words Eq. (8), representing the intersection of \bar{G} and $G = \gamma G(U_k)$, is combined with Eq. (11), representing a point at the direction of V_{k+1} . Therefore, the resulted U_{k+1} will be located on both \bar{G} and $G = \gamma G(U_k)$ and it will also be at the direction of V_{k+1} . This replacement results in

$$(1 - \gamma)G(U_k) + \nabla^T G(U_k)\beta_{k+1}V_{k+1} - \nabla^T G(U_k)U_k = 0 \quad (12)$$

Manipulating the above equation, one can compute reliability index as

$$\beta_{k+1} = \frac{\nabla^T G(U_k)U_k - (1 - \gamma)G(U_k)}{\nabla^T G(U_k)V_{k+1}} \quad (13)$$

By using this value of reliability index, U_{k+1} as the MPP of iteration $k+1$ can be obtained from Eq. (11).

In the above represented algorithm, γ and θ are two adjusting parameters. As explained before, if $\gamma = 0$ and $\theta \rightarrow \infty$ the algorithm reduces to HL-RF. If $\gamma = 0$ and θ can take a finite value, the algorithm becomes similar to what Gong and Yi [28] have suggested. The proposed algorithm is a general method in which two parameters can take different values. Each of the parameters γ and θ is to consider a type of nonlinearity. Parameter γ is for the nonlinearity along $(n+1)$ th axis G , and parameter θ is for the nonlinearity of interactions of random variables in a specific plane (i.e. when G does not change and it takes a fixed value). It will be shown that while HL-RF fails to converge in the cases with high nonlinearity, the adjusting parameters of the proposed algorithm make the convergence possible in such cases.

2.2. Summary

Before going through numerical examples and to clarify the steps of the proposed algorithm, the summary of the algorithm based on previous explanations is expressed in the following step-by-step way:

1. Define LSF in terms of the basic random variables, i.e. write $g(X) = 0$.
2. Use the transformation of HL-RF method to normalize the LSF, i.e. write $G(U) = 0$.
3. Select values for γ and θ ($0 \leq \gamma < 1$ and $\theta > 0$).
4. Select a point for U_1 . Write $\beta_1 = \|U_1\|$ and set $k = 1$.
5. Compute the auxiliary point A_{k+1} from Eq. (9).
6. Determine the direction of U_{k+1} from Eq. (10).
7. Compute β_{k+1} from Eq. (13).
8. Determine U_{k+1} from Eq. (11).
9. Check for the convergence. If the convergence criterion is satisfied go to step 10. Otherwise, set $k = k + 1$ and go to step 5.

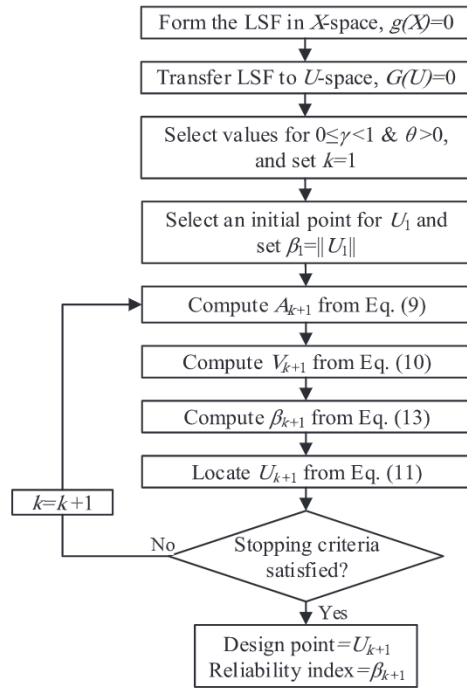


Fig. 4. Flowchart of the proposed algorithm.

10. Write β_{k+1} and U_{k+1} as the final reliability index and design point, respectively.

Flowchart of the proposed algorithm has been also provided in Fig. 4.

3. Numerical examples

In this section, nonlinear examples are selected to demonstrate the performance of the proposed algorithm. In each example, apart from representing the answers of the literature, a table has been presented to reflect the analysis results of the proposed algorithm with various sets of (γ, θ) , evidently among many possible sets. In these tables the sets of (γ, θ) approach the set $(0, \infty)$, corresponding to HL-RF in the last row. Moreover, in each example, the behavior of the proposed algorithm (with one of the applied sets) is compared with that of HL-RF through an illustrative diagram.

Example 1. The nonlinear LSF of this example as a cubic polynomial with mixed term is expressed in the following form

$$g(x) = x_1^3 + x_1^2 x_2 + x_2^3 - 18 \quad (14)$$

where x_1 and x_2 have normal distribution with means $\mu_1 = 10$, $\mu_2 = 9.9$ and standard deviations $\sigma_1 = \sigma_2 = 5$.

According to Wang and Grandhi [24] and Gong et al. [29] reliability index is 2.2983. Keshtegar and Miri [32] and Keshtegar [33] obtained 2.2982 as reliability index. Yang [27] computed this index 2.298. The reliability index computed by MCS and using 10^6 samples is 2.5274. In Table 1, the analysis results of the proposed algorithm with some sets of (γ, θ) have been brought. As it is observed the most conservative set of (γ, θ) among the presented ones of the table, i.e. $(0.9, 0.1)$, corresponds to the largest number of required iterations (136 iterations). By moving downwards in the rows of Table 1, the sets become less conservative and therefore the results show more efficiency such that for the set $(0, 1)$ the proposed algorithm computes $\beta = 2.2983$ after only 8 iterations. The last row of Table 1 provides the least conservative possible set in the proposed algorithm, i.e. $(0, \infty)$, and is corresponding to HL-RF method as a special case of the proposed algorithm. According to this row HL-RF fails to converge. This means the nonlinearity of the LSF of this example does not let θ be infinitively large. Fig. 5 compares the behavior of

Table 1
Results with different sets of (γ, θ) in Example 1.

γ	θ	β	Ite.
0.9	0.1	2.2982	136
0.8	0.2	2.2982	69
0.7	0.3	2.2982	46
0.6	0.4	2.2982	34
0.5	0.5	2.2983	26
0.4	0.6	2.2983	21
0.3	0.7	2.2983	17
0.2	0.8	2.2983	14
0.1	0.9	2.2983	11
0	1	2.2983	8
0	∞	Not converged	

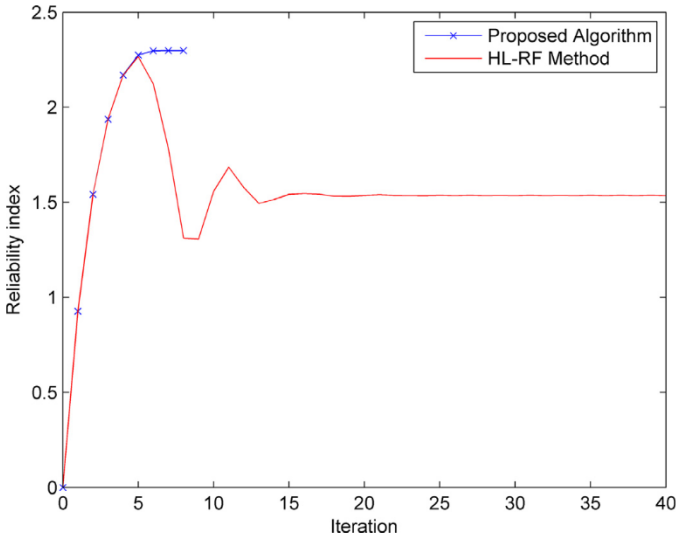


Fig. 5. Iteration history of the proposed method and HL-RF in Example 1.

the proposed algorithm for $(\gamma, \theta)=(0,1)$ with that of HL-RF. While the proposed algorithm is efficient for the aforementioned set of parameters, HL-RF is faced with slight periodic behavior (around 1.5355 and 1.5370) and cannot be stabilized.

Example 2. In this example, the LSF is a quartic polynomial as

$$g(x) = x_1^4 + 2x_2^4 - 20 \quad (15)$$

where x_1 and x_2 have normal distribution with means $\mu_1 = \mu_2 = 10$ and standard deviations $\sigma_1 = \sigma_2 = 5$. This example has been solved by Wang and Grandhi [24] resulting in $\beta = 2.3633$. Yang [27] computed reliability index 2.363. Keshtegar and Miri [32] reached 2.3653 as the answer. Gong et al. [29] solved the example resulting in $\beta = 2.3628$. The answer reported by Pericaro et al. [13] is 2.3655. The reliability index of MCS after the generation of 10^6 samples is 2.9019. According to Table 2, when the set (0.5,0.5) changes to the less conservative one (0.4,0.6) to reach a more efficient solution, divergence is resulted. In such a nonlinear con-

Table 2
Results with different sets of (γ, θ) in Example 2.

γ	θ	β	Ite.
0.9	0.1	2.3654	154
0.8	0.2	2.3654	78
0.7	0.3	2.3654	52
0.6	0.4	2.3655	38
0.5	0.5	2.3655	30
0.4	0.6	Not converged	
0	∞	Not converged	

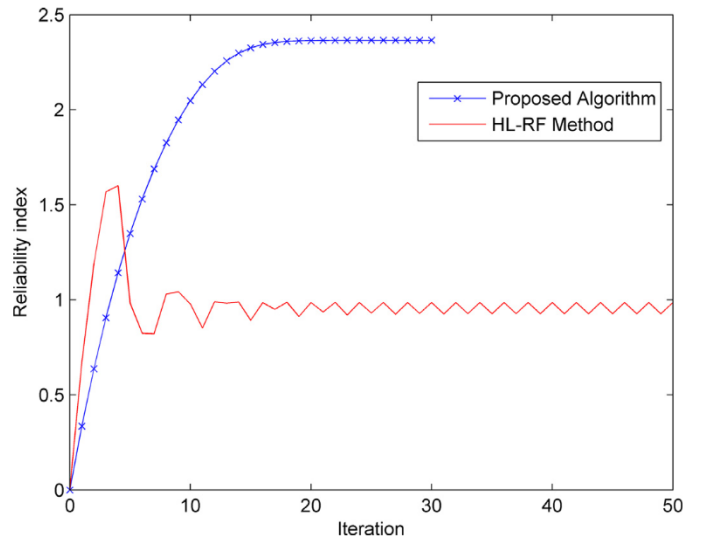


Fig. 6. Iteration history of the proposed method and HL-RF in Example 2.

Table 3
Statistics of random variables in Example 3.

Variable	Distribution	Mean	Standard deviation
x_1	Type II largest value	10	5
x_2	Normal	25	5
x_3	Normal	0.8	0.2
x_4	Lognormal	0.0625	0.0625

dition, it is not surprising to see HL-RF diverged (last row of Table 2). The behaviors of HL-RF and the proposed algorithm for $(\gamma, \theta)=(0.5,0.5)$ have been also illustrated in Fig. 6. The periodic behavior of HL-RF and the effects of applied parameters γ and θ in making HL-RF stable are clearly seen in this figure.

Example 3. The following highly nonlinear LSF is taken from the reliability analysis of a pipeline where the limit state surface was generated using response surface fitting. This LSF is expressed as

$$\begin{aligned} g(x) = & 1.1 - 0.00115x_1x_2 + 0.00157x_2^2 \\ & + 0.00117x_1^2 + 0.0135x_2x_3 - 0.0705x_2 \\ & - 0.00534x_1 - 0.0149x_1x_3 - 0.0611x_2x_4 \\ & + 0.0717x_1x_4 - 0.226x_3 + 0.0333x_3^2 \\ & - 0.558x_3x_4 + 0.998x_4 - 1.339x_4^2 \end{aligned} \quad (16)$$

The statistics of random variables are presented in Table 3. MCS computes reliability index 1.3961 using 10^6 samples. Liu and Kiureghian [23] used merit function to obtain $\beta = 1.36$. The method proposed by Santosh et al. [26] did not give a good answer in this case and computed $\beta = 2.4203$. Yang [27] solved the example resulting in $\beta = 1.330$. Gong and Yi [28] and Keshtegar [33] reached 1.3304 as the answer. Keshtegar and Miri [32] obtained reliability index 1.3305. Gong et al. [29] and Pericaro et al. [13] computed $\beta = 1.3298$ and $\beta = 1.3685$, respectively.

The proposed algorithm has been implemented in this example with some sets of (γ, θ) , as tabulated in Table 4. According to the table, the proposed algorithm reaches $\beta = 1.3304$ with $(\gamma, \theta) = (0.9, 0.1)$ as the most conservative one and $(\gamma, \theta) = (0, 1)$ as the most efficient one (both among the applied sets). However, the last row corresponding to HL-RF cannot converge, a sign indicating θ cannot be arbitrarily selected in this example. In Fig. 7, the periodic behavior of HL-RF has been illustrated. While according to the figure, the proposed algorithm with $(\gamma, \theta) = (0, 1)$ poses an efficient stable behavior.

Example 4. In this example, to test the performance of the proposed algorithm, a highly nonlinear 10-variable LSF including cross-product

Table 4Results with different sets of (γ, θ) in Example 3.

γ	θ	β	Ite.
0.9	0.1	1.3304	112
0.8	0.2	1.3304	57
0.7	0.3	1.3304	37
0.6	0.4	1.3304	27
0.5	0.5	1.3304	20
0.4	0.6	1.3304	18
0.3	0.7	1.3304	17
0.2	0.8	1.3304	15
0.1	0.9	1.3304	14
0	1	1.3304	14
0	∞	Not converged	

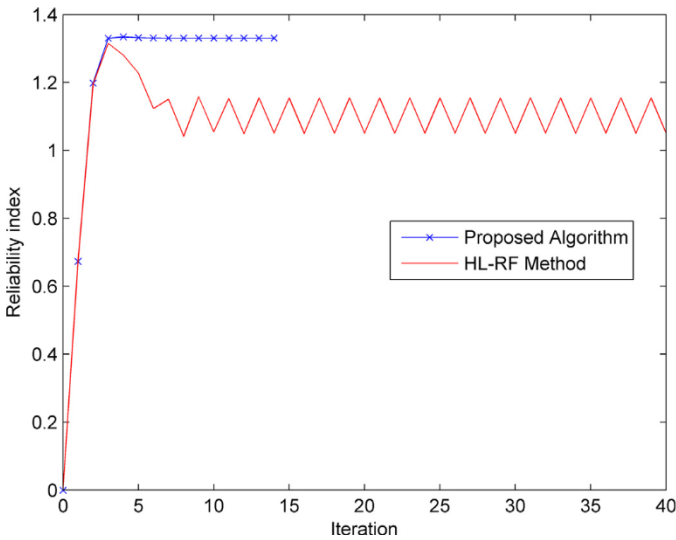


Fig. 7. Iteration history of the proposed method and HL-RF in Example 3.

Table 5Results with different sets of (γ, θ) in Example 4.

γ	θ	β	Ite.
0.9	0.1	3.7515	127
0.8	0.2	3.7515	65
0.7	0.3	3.7515	44
0.6	0.4	3.7515	33
0.5	0.5	3.7515	26
0.4	0.6	3.7515	21
0.3	0.7	3.7515	18
0.2	0.8	3.7515	15
0.1	0.9	3.7515	14
0	1	3.7515	12
0	∞	Not converged	

terms of random variables is designed to be examined. This LSF is defined as

$$g(x) = 2 + 0.015 \left(\sum_{i=1}^9 x_i^2 \right)^3 - x_{10} \quad (17)$$

where all ten variables follow normal distribution with $\mu = 1$ and $\sigma = 0.5$. The reliability index computed by MCS and using 10^6 samples is 4.4651. Table 5 summarizes the results taken from the proposed algorithm for various values of adjusting parameters. In the last row of the table, the divergence of HL-RF has been mentioned. Chaotic behavior of HL-RF and the stability and efficiency of the proposed algorithm for $(\gamma, \theta) = (0, 1)$ have been illustrated in Fig. 8.

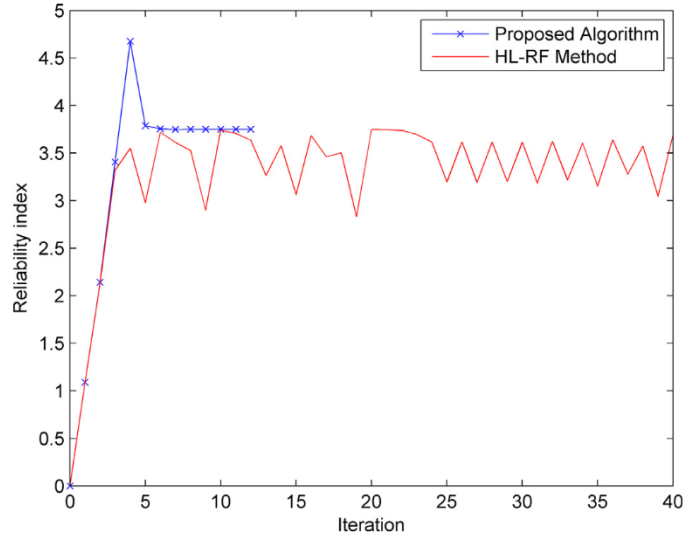


Fig. 8. Iteration history of the proposed method and HL-RF in Example 4.

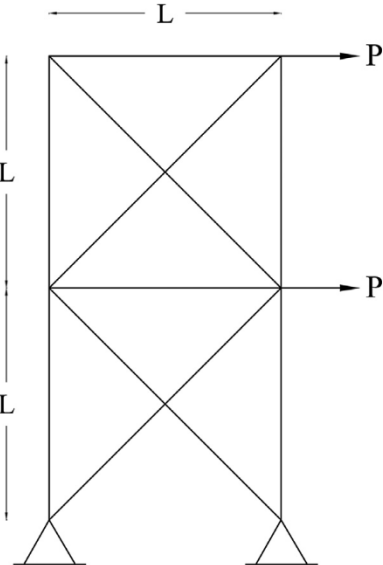


Fig. 9. 10-bar truss structure of Example 5.

Table 6

Statistics of random variables in Example 5.

Variable	Distribution	Mean	Standard deviation
A_1 (m^2)	Normal	10^{-2}	5×10^{-4}
A_2 (m^2)	Normal	1.5×10^{-3}	7.5×10^{-5}
A_3 (m^2)	Normal	6×10^{-3}	3×10^{-4}
B	Normal	1	0.1
P (N)	Gumbel	2.5×10^5	2.5×10^4
E (MPa)	Lognormal	6.9×10^4	3.45×10^3

Example 5. This example studies the 10-bar truss structure of Fig. 9. The vertical, horizontal and diagonal truss members are aluminum rods with three different cross-sectional areas A_1 , A_2 and A_3 , respectively. In this structure, the diagonal members do not intersect at the intersection points. The structure is subjected to external loads P . The implicit LSF of the structure is considered the time the horizontal displacement at the upper right corner of the truss structure exceeds allowable displacement $d_0 = 0.1$ m.

The statistics of the random variables are presented in Table 6 and L is considered deterministic with the value of 9 m. After generation

Table 7

Results with different sets of (γ, θ) in Example 5.

γ	θ	β	Ite.
0.9	0.1	4.3006	173
0.8	0.2	4.3006	96
0.7	0.3	4.3005	68
0.6	0.4	4.3005	54
0.5	0.5	4.3005	45
0.4	0.6	4.3005	39
0.3	0.7	4.3005	35
0.2	0.8	4.3005	31
0.1	0.9	4.3005	29
0	1	4.3005	27
0	∞	4.3005	6

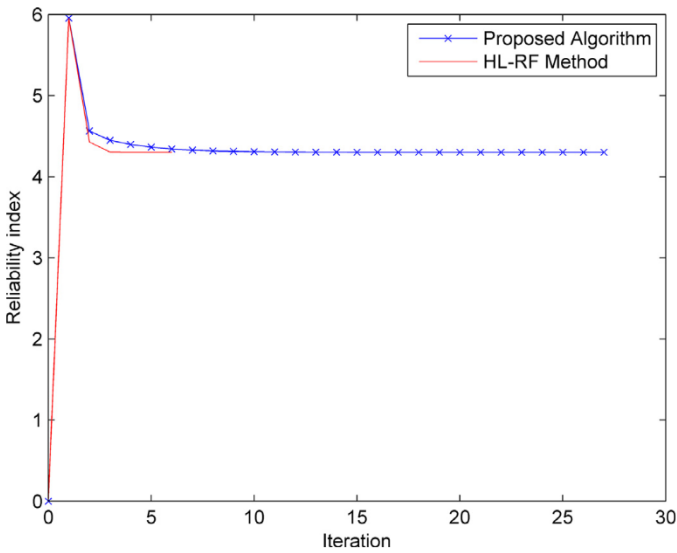


Fig. 10. Iteration history of the proposed method and HL-RF in Example 5.

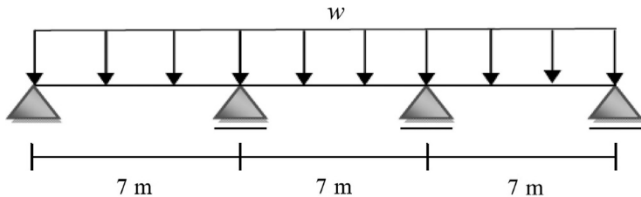


Fig. 11. Three-span continuous beam of Example 6.

of 1.7×10^9 samples, MCS gives 4.4937 as reliability index. Naess et al. [8] solved this example and obtained reliability index 4.5195. Keshtegar and Miri [32] analyzed this truss and computed $\beta = 4.2994$.

The results of the proposed algorithm for various values of adjusting parameters are presented in Table 7 with the last row as the results of HL-RF. This table shows that in all cases, including HL-RF case, the convergence has been resulted. This example confirms the fact that if HL-RF can converge, it occurs with the fastest speed (only 6 iterations in this example). The convergence of HL-RF and the proposed algorithm for $(\gamma, \theta) = (0, 1)$ have been illustrated in Fig. 10.

Example 6. The three-span continuous beam of Fig. 11 is designed to be considered in this example.

The LSF corresponding to the deflection of this structure is defined as follows

$$g(w, E, h) = \frac{7}{360} - 360 \frac{w}{Eh^4} \quad (18)$$

Table 8

Statistics of random variables in Example 6.

Variable	Distribution	Mean	Standard deviation
w (kN/m)	Normal	10	0.4
E (kN/m ²)	Normal	2×10^7	0.5×10^7
h (m)	Normal	0.4	0.01

Table 9

Results with different sets of (γ, θ) in Example 6.

γ	θ	β	Ite.
0.9	0.1	2.5217	78
0.8	0.2	2.5216	60
0.7	0.3	2.5216	43
0.6	0.4	2.5216	34
0.5	0.5	2.5216	29
0.4	0.6	2.5216	24
0.3	0.7	Not converged	
0	∞	Not converged	

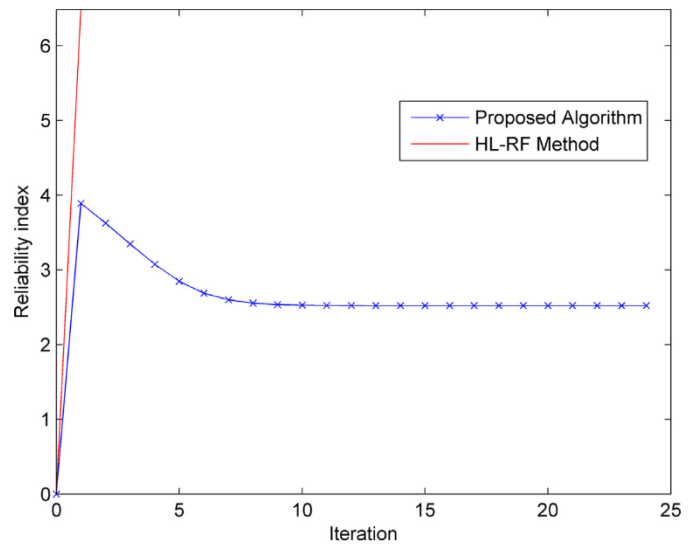


Fig. 12. Iteration history of the proposed method and HL-RF in Example 6.

where w , E and h are the intensity of the uniform load, modulus of elasticity and height of the T-shaped section, respectively (all defined in Table 8). The reliability index MCS computes after the generation of 10^6 samples is 3.4765.

Table 9 provides the final answers of the proposed algorithm for some values of adjusting parameters. As it can be observed in the table, $(\gamma, \theta) = (0.4, 0.6)$ results in an efficient solution (using 24 iterations). This table shows that (γ, θ) should be more conservative than $(0.3, 0.7)$. In fact the high nonlinearity of the LSF causes the insufficiently conservative set $(0.3, 0.7)$ to diverge. According to the last row of Table 9, HL-RF diverges, too. In Fig. 12, the efficiency of the proposed algorithm for the appropriate set $(\gamma, \theta) = (0.4, 0.6)$ can be observed, while according to the figure β in HL-RF rapidly increases with a steep slope.

Example 7. In this example, a highly nonlinear LSF as a severe test for the proposed algorithm has been provided [34]. This LSF corresponds to a two-degree-of-freedom primary-secondary dynamic system, as depicted in Fig. 13.

According to the paper proposed by Kiureghian and Stefano [34] the LSF can be expressed by eight random variables, including the masses m_p and m_s , spring stiffnesses k_p and k_s , damping ratios ζ_p and ζ_s , the force capacity of the secondary spring F_s , and the intensity of a white-noise base excitation of the system S_0 . In these random variables, the

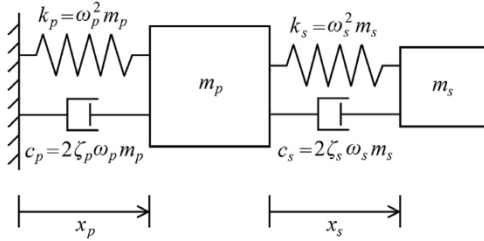


Fig. 13. Primary-secondary system of Example 7.

Table 10
Statistics of random variables in Example 7.

Variable	Distribution	Mean	Standard deviation
m_p	Lognormal	1	0.1
m_s	Lognormal	0.01	0.001
k_p	Lognormal	1	0.2
k_s	Lognormal	0.01	0.002
ζ_p	Lognormal	0.05	0.02
ζ_s	Lognormal	0.02	0.01
F_s	Lognormal	15	1.5
S_0	Lognormal	100	10

Table 11
Results with different sets of (γ, θ) in Example 7.

γ	θ	β	Ite.
0.9	0.1	2.1231	109
0.8	0.2	2.1231	55
0.7	0.3	Not converged	
0	∞	Not converged	

subscripts p and s denote the primary and secondary oscillators, respectively. The statistics of eight aforementioned random variables are listed in Table 10.

As Kiureghian and Stefano [34] have shown, the mean square relative displacement response of the secondary spring to the white-noise base excitation, i.e. $E(x_s^2)$, can be written as

$$E(x_s^2) = \frac{\pi S_0}{4\zeta_s \omega_s^3} \left[\frac{\zeta_a \zeta_s}{\zeta_p \zeta_s (4\xi_a^2 + \eta^2) + v \xi_a^2} \frac{(\zeta_p \omega_p^3 + \zeta_s \omega_s^3) \omega_p}{4 \zeta_a \omega_a^4} \right] \quad (19)$$

and the LSF can be expressed as

$$g = F_s - k_s p [E(x_s^2)]^{1/2} \quad (20)$$

In the above equations, $\omega_p = (k_p/m_p)^{0.5}$ and $\omega_s = (k_s/m_s)^{0.5}$ are natural frequencies of the primary and secondary oscillators, respectively. $\omega_a = (\omega_p + \omega_s)/2$ and $\zeta_a = (\zeta_p + \zeta_s)/2$ are the average frequency and damping ratio, respectively. $v = m_s/m_p$ is the mass ratio, $\eta = (\omega_p - \omega_s)/\omega_a$ is a tuning parameter, and p is a deterministic peak factor equal to 3.

MCS computes $\beta = 2.7360$ after the generation of 10^6 samples. According to the answer extracted from Kiureghian and Stefano [34] reliability index is 2.12. Keshtegar [33] reported 2.0163 as reliability index. According to Table 11, even $(\gamma, \theta) = (0.7, 0.3)$ is not appropriate for convergence. This is a sign of extreme nonlinearity of the present LSF. However, even in such a nonlinear problem, the proposed algorithm is capable of posing a stable solution and finding the answer. This occurs by assigning appropriate values to the adjusting parameters, as tabulated in two beginning rows of Table 11. It should be noted that there are also more appropriate sets than $(0.8, 0.2)$ of second row resulting in better efficiency. As an example, the set $(0.7, 0.225)$ results in convergence after only 29 iterations. Capability of handling such a problem is a sign of robustness of the proposed algorithm. Fig. 14 provides the behavior of HL-RF and the proposed algorithm for $(\gamma, \theta) = (0.8, 0.2)$. Extreme nonlinearity of the LSF is clearly seen through the chaotic behavior of

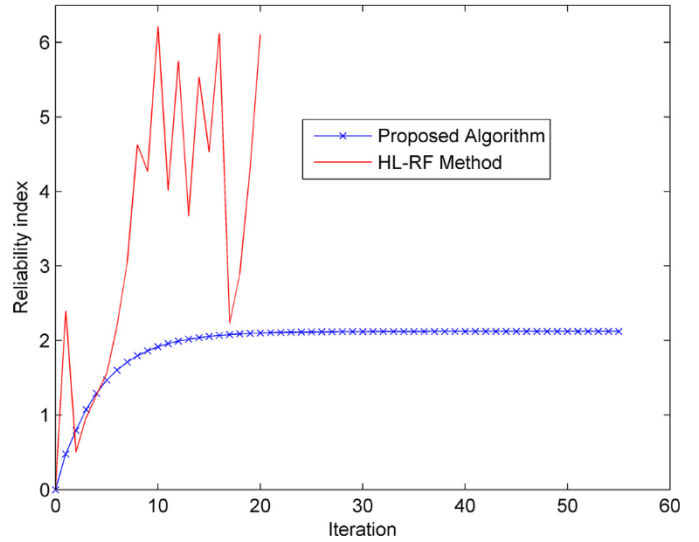


Fig. 14. Iteration history of the proposed method and HL-RF in Example 7.

HL-RF in this figure. However, the curve corresponding to the proposed algorithm is completely stable.

4. Discussion

In the previous section, seven reliability examples were proposed. Each example was analyzed by using the proposed algorithm and with various sets of introduced adjusting parameters, represented in a corresponding table. Besides, the results of the analysis of each example were compared with those of HL-RF through illustrative diagrams. According to the tables and diagrams, HL-RF is not successful in the presented numerical examples. As a matter of fact, apart from Example 5, HL-RF fails to converge in other six examples. However, the proposed algorithm has shown its robustness in all numerical examples. Since HL-RF is itself a special case of the proposed algorithm, it can be concluded that in the aforementioned six examples, either γ should not be as small as zero or θ should not be as large as infinity. For instance, in Examples 1, 3 and 4, γ can take its minimum possible value for convergence, as it is seen in the corresponding tables that the set $(\gamma, \theta) = (0, 1)$ can result in convergence, but infinitely large values of θ cannot work. According to Tables 2, 9 and 11, respectively corresponding to Examples 2, 6 and 7, neither γ can be arbitrarily small nor can θ be arbitrarily large. Example 5 is the only presented example in which HL-RF successfully finds the answer and any set of (γ, θ) can also be applied. However, different selections of the parameters cause different efficiencies. This example confirms the fact that HL-RF is the fastest method provided that it can overcome convergence difficulties. This fact can be also inferred using the concepts of the proposed algorithm. Indeed, since HL-RF is a special case of the proposed algorithm with the largest possible step lengths, i.e. $\gamma = 0$ and $\theta \rightarrow \infty$, its high convergence speed is understandable.

Thus, the appropriate selection of the adjusting parameters of the proposed algorithm can guarantee the convergence of the method. Referring to the illustrative diagrams and comparing the results of the proposed algorithm and HL-RF, one can see how stable and reliable the proposed algorithm acts due to the insertion of adjusting parameters. In addition, from the tables of analysis results, it can be observed that the proposed algorithm can also work efficiently. These all approve the positive effects of introducing the aforementioned parameters as control parameters of convergence and efficiency. In order to see the accuracy and efficiency of the proposed algorithm conveniently, Table 12 has been provided. In this table, reliability index and iterations of the proposed algorithm for a set of adjusting parameters are compared with the results of HL-RF method and MCS. Besides, the last

Table 12
Comparison of analysis results in numerical examples.

Ex.	Proposed method			HL-RF		MCS		β in the literature	
	γ	θ	β	Ite.	β	Ite.	β	Samples	
1	0	1	2.2983	8	No convergence		2.5274	10^6	-2.2983, Wang and Grandhi [24] -2.298, Yang [27] -2.2982, Keshtegar and Miri [32] -2.2983, Gong et al. [29] -2.2982, Keshtegar [33] -2.3633, Wang and Grandhi [24] -2.363, Yang [27]
2	0.5	0.5	2.3655	30	No convergence		2.9019	10^6	-2.3653, Keshtegar and Miri [32] -2.3628, Gong et al. [29] -2.3655, Pericaro et al. [13] -1.36, Liu and Kiureghian [23] -2.4203, Santosh et al. [26] -1.330, Yang [27] -1.3304, Gong and Yi [28]
3	0	1	1.3304	14	No convergence		1.3961	10^6	-1.3305, Keshtegar and Miri [32] -1.3298, Gong et al. [29] -1.3685, Pericaro et al. [13] -1.3304, Keshtegar [33]
4	0	1	3.7515	12	No convergence		4.4651	10^6	-
5	0	1	4.3005	27	4.3005	6	4.4937	1.7×10^9	-4.5195, Naess et al. [8] -4.2994, Keshtegar and Miri [32]
6	0.4	0.6	2.5216	24	No convergence		3.4765	10^6	-
7	0.8	0.2	2.1231	55	No convergence		2.7360	10^6	-2.12, Kiureghian and Stefano [34] -2.0163, Keshtegar [33]

column of Table 12 shows the reliability index of some other papers of the literature. Since Examples 4 and 6 are designed by the authors, in the last column (corresponding to the literature) there is no reference. What should be noted about this table is that the final answer of the proposed method may differ from that of MCS (like Example 1). This should not be attributed to the errors because it stems from different definitions. In the proposed algorithm the purpose is to determine the minimum distance of limit state surface from the origin of U -space in the geometric sense (as defined by Hasofer and Lind [21]). However, the purpose in simulation methods is to find probability of failure, and then reliability index is just reported by using the famous relation of FORM, i.e. $\beta = -\Phi^{-1}(P_f)$. Hence, this may differ, in some nonlinear cases, from the common reliability index defined by Hasofer and Lind. Thus, in such cases, it would be better to compare the reliability index of the proposed algorithm (as an approximation method) with this index in the methods looking for the aforementioned minimum distance (i.e. with reliability index of other approximation methods).

Based on the above explanations and the illustrative diagrams and tables, HL-RF has difficulty in convergence and it cannot get rid of periodic or chaotic behaviors in many numerical examples. These instabilities are associated with the nonlinearity of the limit state functions. Since nonlinearity is strongly tied to a vast part of engineering relations, HL-RF is not applicable in many engineering problems. The proposed algorithm can deal with this nonlinearity challenge and therefore provides a choice to be applied in engineering and reliability problems.

5. Conclusion

In this paper, a reliability algorithm as the generalization of HL-RF has been proposed. In comparison with HL-RF, the proposed algorithm benefits from two significant adjusting parameters by which controlling the convergence sequence in highly nonlinear cases becomes possible. The parameters improve the robustness of HL-RF and are applied to deal with the instability observed in HL-RF. It has been shown that two parameters are corresponding to step lengths in two different directions and the proposed algorithm reduces to HL-RF when both step lengths take the extreme values in their defined ranges. Although the proposed

algorithm is as simple as HL-RF to implement, it is more robust due to the contribution of adjusting parameters. Through nonlinear numerical examples, the robustness and efficiency of the proposed algorithm have been shown.

Acknowledgements

The authors would like to acknowledge all supports from [Iran University of Science and Technology](#). This research did not receive any specific grant from funding agencies in the public, commercial, or not-for-profit sectors.

References

- [1] Rackwitz R. Reliability analysis-a review and some perspectives. Struct Saf 2001;23(4):365–95. [http://dx.doi.org/10.1016/S0167-4730\(02\)00009-7](http://dx.doi.org/10.1016/S0167-4730(02)00009-7).
- [2] Chowdhury R, Adhikari S. Reliability analysis of uncertain dynamical systems using correlated function expansion. Int J Mech Sci 2011;53(4):281–5. <http://dx.doi.org/10.1016/j.ijmecsci.2011.01.009>.
- [3] Shayanfar MA, Barkhordari MA, Roudak MA. Locating design point in structural reliability analysis by introduction of a control parameter and moving limited regions. Int J Mech Sci 2017;126:196–202. <http://dx.doi.org/10.1016/j.ijmecsci.2017.04.003>.
- [4] Wang L, Grandhi RV. Efficient safety index calculation for structural reliability analysis. Comput Struct 1994;52(1):103–11. [http://dx.doi.org/10.1016/0045-7949\(94\)90260-7](http://dx.doi.org/10.1016/0045-7949(94)90260-7).
- [5] Mishra SK, Roy BK, Chakraborty S. Reliability-based-design-optimization of base isolated buildings considering stochastic system parameters subjected to random earthquakes. Int J Mech Sci 2013;75:123–33. <http://dx.doi.org/10.1016/j.ijmecsci.2013.06.012>.
- [6] Shayanfar MA, Barkhordari MA, Roudak MA. An adaptive importance-sampling-based algorithm using the first-order method for structural reliability. Int J Optim Civ Eng 2017;7(1):93–107.
- [7] Yu Q, Nosonovsky M, Esche SK. Monte Carlo simulation of grain growth of single-phase systems with anisotropic boundary energies. Int J Mech Sci 2009;51(6):434–42. <http://dx.doi.org/10.1016/j.ijmecsci.2009.03.011>.
- [8] Naess A, Leira BJ, Batsevych O. System reliability analysis by enhanced Monte Carlo simulation. Struct Saf 2009;31:349–55. <http://dx.doi.org/10.1016/j.strusafe.2009.02.004>.
- [9] Jahani E, Muhamma RL, Shayanfar MA, Barkhordari MA. Reliability assessment with fuzzy random variables using interval Monte Carlo simulation. Computer-Aided Civil and Infrastructure Engineering 2014;29(3):208–20. <http://dx.doi.org/10.1111/mice.12028>.
- [10] Ossai CI, Boswell B, Davis LJ. Application of Markov modelling and Monte Carlo simulation technique in failure probability estimation—a consideration of cor-

- rosion defects of internally corroded pipelines. Eng Fail Anal 2016;68:159–71. <http://dx.doi.org/10.1016/j.englfailanal.2016.06.004>.
- [11] Zhao YG, Lu ZH. Fourth-moment standardization for structural reliability assessment. J Struct Eng 2007;133(7):916–24. [http://dx.doi.org/10.1061/\(ASCE\)0733-9445\(2007\)133:7\(916\)](http://dx.doi.org/10.1061/(ASCE)0733-9445(2007)133:7(916)).
- [12] Du X, Hu Z. First order reliability method with truncated random variables. J Mech Des 2012;134(9). 091005–091005–9 <http://dx.doi.org/10.1115/1.4007150>.
- [13] Pericaro GA, Santos SR, Ribeiro AA, Matioli LC. HLRF-BFGS optimization algorithm for structural reliability. Appl Math Model 2015;39(7):2025–35. <http://dx.doi.org/10.1016/j.apm.2014.10.024>.
- [14] Alibrandi U, Koh C. First-order reliability method for structural reliability analysis in the presence of random and interval variables. J Risk Uncertainty 2015;1(4):1–10. <http://dx.doi.org/10.1115/1.4030911>.
- [15] Grooteman F. Adaptive radial-based importance sampling method for structural reliability. Struct Saf 2008;30:533–42. <http://dx.doi.org/10.1016/j.strusafe.2007.10.002>.
- [16] Jahani E, Shayanfar MA, Barkhordari MA. A new adaptive importance sampling Monte Carlo method for structural reliability. KSCE J Civil Eng 2013;17(1):210–15. <http://dx.doi.org/10.1007/s12205-013-1779-6>.
- [17] Shayanfar MA, Barkhordari MA, Roudak MA. An efficient reliability algorithm for locating design point using the combination of importance sampling concepts and response surface method. Commun Nonlinear Sci Numer Simulat 2017;47:223–37. <http://dx.doi.org/10.1016/j.cnsns.2016.11.021>.
- [18] Cao Z, Dai H, Wang W. Low-discrepancy sampling for structural reliability sensitivity analysis. Struct Eng Mech 2011;38(1):125–40. <http://dx.doi.org/10.12989/sem.2011.38.1.125>.
- [19] Lim J, Lee B, Lee I. Post optimization for accurate and efficient reliability-based design optimization using second-order reliability method based on importance sampling and its stochastic sensitivity analysis. Int J Numer Methods Eng 2016;107(2):93–108. <http://dx.doi.org/10.1002/nme.5150>.
- [20] Yang X, Liu Y, Gao Y. Unified reliability analysis by active learning Kriging model combining with random-set based Monte Carlo simulation method. Int J Numer Methods Eng 2016;108(11):1343–61. <http://dx.doi.org/10.1002/nme.5255>.
- [21] Hasofer AM, Lind NC. Exact and invariant second-moment code format. J Eng Mech Div 1974;100(1):111–21.
- [22] Rackwitz R, Fiessler B. Structural reliability under combined random load sequences. Comput Struct 1978;9(5):489–94. [http://dx.doi.org/10.1016/0045-7949\(78\)90046-9](http://dx.doi.org/10.1016/0045-7949(78)90046-9).
- [23] Liu PL, Kiureghian AD. Optimization algorithms for structural reliability. Struct Saf 1991;9(3):161–77. [http://dx.doi.org/10.1016/0167-4730\(91\)90041-7](http://dx.doi.org/10.1016/0167-4730(91)90041-7).
- [24] Wang L, Grandhi RV. Safety index calculation using intervening variables for structural reliability analysis. Comput Struct 1996;59(6):1139–48. [http://dx.doi.org/10.1016/0045-7949\(96\)00291-X](http://dx.doi.org/10.1016/0045-7949(96)00291-X).
- [25] Elegbede C. Structural reliability assessment based on particles swarm optimization. Struct Saf 2005;27:171–86. <http://dx.doi.org/10.1016/j.strusafe.2004.10.003>.
- [26] Santosh TV, Saraf RK, Ghosh AK, Kushwaha HS. Optimum step length selection rule in modified HL-RF method for structural reliability. Int J Pressure Vessels Piping 2006;83(10):742–8. <http://dx.doi.org/10.1016/j.ijpv.2006.07.004>.
- [27] Yang D. Chaos control for numerical instability of first order reliability method. Commun Nonlinear Sci Numer Simulat 2010;15(10):3131–41. <http://dx.doi.org/10.1016/j.cnsns.2009.10.018>.
- [28] Gong JX, Yi P. A robust iterative algorithm for structural reliability analysis. Struct Multidisc Optim 2011;43:519–27. <http://dx.doi.org/10.1007/s00158-010-0582-y>.
- [29] Gong JX, Yi P, Zhao N. Non-gradient-based algorithm for structural reliability analysis. J Eng Mech 2014;140(6):1–16. [http://dx.doi.org/10.1061/\(ASCE\)EM.1943-7889.0000722](http://dx.doi.org/10.1061/(ASCE)EM.1943-7889.0000722).
- [30] Kamiński M. The Stochastic Perturbation Method for Computational Mechanics. Wiley; 2013.
- [31] Kamiński M, Świdta P. Structural stability and reliability of the underground steel tanks with the stochastic finite element method. Arch Civil Mech Eng 2015;15(2):593–602. <http://dx.doi.org/10.1016/j.acme.2014.04.010>.
- [32] Keshtegar B, Miri M. An enhanced HL-RF method for the computation of structural failure probability based on relaxed approach. Civil Eng Infrastruct 2013;1(1):69–80. <http://dx.doi.org/10.7508/CEIJ.2013.01.005>.
- [33] Keshtegar B. Chaotic conjugate stability transformation method for structural reliability analysis. Comput Methods Appl Mech Eng 2016;310:866–85. <http://dx.doi.org/10.1016/j.cma.2016.07.046>.
- [34] Kiureghian AD, Stefano MD. Efficient algorithm for second-order reliability analysis. J Eng Mech 1991;117(12):2904–23. [http://dx.doi.org/10.1061/\(ASCE\)0733-9399\(1991\)117:12\(2904\)](http://dx.doi.org/10.1061/(ASCE)0733-9399(1991)117:12(2904).

